3-D finite element model of the impaction of a press-fitted femoral stem under various biomechanical environments

Anne-Sophie Poudrel, Arthur Bouffandeau, Giuseppe Rosi, Arnaud Dubory, Charles-Henri Flouzat Lachaniette, Vu-Hieu Nguyen, Guillaume Haiat

▶ **To cite this version:**

Anne-Sophie Poudrel, Arthur Bouffandeau, Giuseppe Rosi, Arnaud Dubory, Charles-Henri Flouzat Lachaniette, et al.. 3-D finite element model of the impaction of a press-fitted femoral stem under various biomechanical environments. Computers in Biology and Medicine, 2024, 174, pp.108405. 10.1016/j.compbiomed.2024.108405 . hal-04601538

HAL Id: hal-04601538
https://hal.science/hal-04601538v1

Submitted on 5 Jun 2024

HAL is a multi-disciplinary open access archive for the deposit and dissemination of scientific research documents, whether they are published or not. The documents may come from teaching and research institutions in France or abroad, or from public or private research centers.

L'archive ouverte pluridisciplinaire **HAL**, est destinée au dépôt et à la diffusion de documents scientifiques de niveau recherche, publiés ou non, émanant des établissements d'enseignement et de recherche français ou étrangers, des laboratoires publics ou privés.

3-D finite element model of the impaction of a press-fitted femoral stem under various biomechanical environments

Anne-Sophie Poudrel[a], Arthur Bouffandeau[a], Giuseppe Rosi[b], Arnaud Dubory[c], Charles-Henri Flouzat Lachaniette[c], Vu-Hieu Nguyen[b], Guillaume Haiat[a,*]

[a] *CNRS, Univ Paris Est Creteil, Univ Gustave Eiffel, UMR 8208, MSME, F-94010 Créteil, France*
[b] *Univ Paris Est Creteil, Univ Gustave Eiffel, CNRS, UMR 8208, MSME, F-94010 Créteil, France*
[c] *Service de Chirurgie Orthopédique et Traumatologique, Hôpital Henri Mondor AP-HP, CHU Paris 12, Université Paris-Est, Créteil, France*

Abstract

Background: Uncemented femoral stem insertion into the bone is achieved by applying successive impacts on an inserter tool called "ancillary". Impact analysis has shown to be a promising technique to monitor the implant insertion and to improve its primary stability.

Method: This study aims to provide a better understanding of the dynamic phenomena occurring between the hammer, the ancillary, the implant and the bone during femoral stem insertion, to validate the use of impact analyses for implant insertion monitoring. A dynamic 3-D finite element model of the femoral stem insertion *via* an impaction protocol is proposed. The influence of the trabecular bone Young's modulus (E_t), the interference fit (IF), the friction coefficient at the bone-implant interface (μ) and the impact velocity (v_0) on the implant insertion and on the impact force signal is evaluated.

Results: For all configurations, a decrease of the time difference between the two first peaks of the impact force signal is observed throughout the femoral stem insertion, up to a threshold value of 0.23 ms. The number of impacts required to reach this value depends on E_t, v_0 and IF and varies between 3 and 8 for the set of parameters considered herein. The bone-implant contact ratio reached after ten impacts varies between 60% and 98%, increases as a function of v_0 and decreases as a function of IF, μ and E_t.

Conclusion: This study confirms the potential of an impact analyses-based method to monitor implant insertion and to retrieve bone-implant contact properties.

Keyword: femoral stem, finite element analysis, dynamic modeling, impact analysis, friction coefficient, interference fit, Young's modulus, bone-implant contact

*Corresponding author: guillaume.haiat@cnrs.fr

1. Introduction

Total hip arthroplasty (THA) is one of the most frequent orthopaedic surgeries. More than 150 000 operations are performed in France yearly [1] and this number is expected to rise due to population's aging. Such surgery aims at replacing the dysfunctional joint to relieve pain and recover the loss of mobility due to degenerative joint disease (e.g. arthrosis) [2] or traumatic injury. Currently, the surgeons use both cemented and uncemented procedures. While the first technique is the oldest and uses cement to provide the initial fixation of the implant into the bone, uncemented procedures, which consist of inserting the implant directly in contact with the bone are developing fast. Cemented procedures are interesting for patients with poor bone quality, but allergic responses and shocks due to the detachment of cement particles are widely reported in the literature, which are the important reasons for revisions [3]. Interestingly, uncemented techniques foster bone remodeling at the bone-implant interface and increase the long-term success of the surgery when performed properly. The success of uncemented surgeries depends on the implant primary stability, achieved during the surgery [4]. In particular, the femoral stem is inserted into a slightly undersized bone cavity previously prepared by the surgeon, by applying successive impacts on the upper surface of an inserter tool called "ancillary", which is temporary fixed to the implant during the insertion. An important challenge for the surgeon is to adapt the impaction protocol to reach sufficient initial mechanical fixation, thanks to press-fit phenomena, while avoiding excessive stresses at the bone-implant interface [5]. Reaching this compromise is tricky since it depends on several parameters related to the patient, the implant or the surgical protocol. Currently, the surgeons relies on their proprioception to adapt the impaction procedure, which is subjective and may lead to failures due to aseptic loosening [6] or periprosthetic fractures [7]. A method allowing to assess implant stability would therefore be useful to improve the surgical procedure.

Among the different vibro-acoustic methods under development [8, 9, 10], impact analysis has shown to be a promising non-destructive and quantitative technique to estimate acetabular cup implant stability [11, 12, 13, 14] and monitor femoral stem insertion [15, 16, 17]. The method consists in analyzing the temporal variation of the impact force applied by the hammer on the ancillary during the implant insertion. In particular, a temporal indicator was derived from this force signal [15, 16, 17] to indicate the femoral stem insertion end-point, which is defined as the insertion step that maximizes initial fixation while avoiding periprosthetic fracture. This indicator, which corresponds to the time difference between the two first peaks of the impact force signal [15], was shown to be in agreement with the surgeon proprioception in previous *in vitro* [15] and

ex vivo studies on bovine femurs [16] and anatomical subjects [17]. However, several phenomena should be clarified for an optimal application of this method in the clinic. First, the sensitivity of the indicator to the bone-implant contact (BIC) ratio, which plays an important role on the implant stability [18], could not be retrieved experimentally [15, 16, 17]. Second, the influence of various biomechanical parameters (*i.e.* bone geometrical and material properties), along with the influence of the surgical procedure (*i.e* impact number and velocity, implant geometry and material) on the impact force signals remains unclear. Due to the varying physical characteristics of bone tissues and to the difficulty to measure the BIC ratio experimentally, the use of numerical simulations is the most adapted approach to address these issues.

In the literature, many numerical studies focused on the femoral stem stability by considering the evaluation of the contact pressure [19] or the estimation of the micromotions at the bone-implant interface during daily activities such as stair climbing [18, 20] or walking [21, 22]. These analyses give good insights on the influence of the implant design geometry [23, 24] and material properties, the patient bone quality [25], the bone-implant contact ratio [18] or the bone cavity size geometry [19] on the implant primary and/or secondary stability [26]. However, these studies did not investigate the implant impaction process itself -which determines the success of uncemented surgeries [5]-, since they were performed on the femoral stem already inserted into the bone cavity. In this context, previous studies by our group investigated the biomechanical phenomena occurring during the press-fit quasi-static insertion of both uncemented Acetabular Cup Implants (ACI) [27, 28] and femoral stems [29]. The influence of the bone Young's modulus, of the bone-implant friction coefficient and of the interference fit on both the implant insertion and the primary stability was analyzed. While these studies [27, 28, 29] are relevant to understand the determinants of implant stability, they do not provide information on the dynamic phenomena occurring during the insertion and in particular, on the temporal variation of the impact force signal. Very few dynamic simulations of uncemented implant insertion are proposed in the literature. Michel et al. [30] developed a dynamic finite element model of the ACI impaction and validated the use of impact analysis to predict the bone-implant contact area of an ACI. However, such study has not yet been performed for the femoral stem. A uni-axial model of the femoral stem impaction configuration was developed by Bishop et al. [31] including the hammer, the ancillary, the femoral stem and the bone, modeled by discrete masses connected by linear elastic springs. However, this model is not based on finite element modeling and two limiting points for its application may be raised. First, the geometry of the bone-implant system was not studied, which prevents analysing

of the stress field at the bone-implant interface. Second, the bone-implant interface was modeled by linear springs, which does not allow to quantify the bone-implant contact ratio, which plays an crucial role on the primary and secondary stability. Interestingly, Monea et al. [32] investigated the influence of femoral stem geometry and press-fit conditions on the evolution and distribution of the bone-implant contact, stresses and strains during and after the hip stem insertion by means of a dynamic analysis. Moreover, bone damage during impaction was studied. However, the impact force features and their variation during impaction were not studied.

The aim of this study is twofold. The first objective is to investigate the variation of the impact force over time during femoral stem insertion in order to validate the use of impact analyses to monitor femoral stem insertion. The second objective is to quantify the influence of varying parameters such as the impact velocity, the bone Young's modulus, the friction coefficient at the bone-implant interface and the interference fit on the implant stability, represented by the bone-implant contact ratio. For that purpose, a three-dimensional finite element nonlinear dynamic analysis of the insertion procedure using successive impacts is developed. The originality of the study is to quantify the effects of various biomechanical parameters on the impact force signal and on the implant stability in order to optimize the impaction protocol, using a realistic geometry of the femoral stem. In particular, the variation of the indicator D, derived from the impact force signal and developed in previous experimental studies [15, 16, 17] will be studied as a function of i) the impact number, ii) the bone-implant contact ratio and iii) the biomechanical configuration.

2. Material and methods

2.1. Finite element model

A 3-D finite element model was used to simulate the insertion of the femoral stem into the bone by successive hammer impacts similarly as in the experiments described in [15] and [10] and schematized in Fig. 1a. Figure 1b shows the geometry of the problem, which consists in five domains: the hammer Ω_h, the ancillary Ω_a, the implant Ω_i and the bone specimen composed of two subdomains: the trabecular bone Ω_{tb} and the cortical bone Ω_{cb}. The ancillary was modeled as a cylinder with the same shape and dimensions as in [29, 10] (outer radius of 16 mm, length of 180 mm) and it was bonded to the femoral stem. The choice of the implant geometry, the bone cavity size and the interference fit were validated by two experienced surgeons. The FS geometry was created from the STL file of a scan of the FS RMIS implant of size 9 (CERAFIT RMIS, Ceraver, Roissy, France). The bone specimen was designed as a cylinder of 110 mm length and

20 mm radius, with an outer layer of 3.5 mm of thickness corresponding to the cortical bone, the inner cylinder representing the trabecular bone. The distal part of the femur was neglected in the model to represent the *in vitro* tests described in [15, 10]. A bone cavity was created in ANSYS workbench (v.20, ANSYS Inc., Canonsburg, PA, USA) by boolean subtraction of the rasp volume, similarly as in [29]. The rasp's geometry corresponds to the FS's one, undersized with a scale factor. The diameter difference between the rasp and the implant is called the interference fit IF. Eventually, the full geometry was reduced to a symmetric model following the plane of symmetry of the implant, corresponding to the (XZ) plane (see Fig. 1).

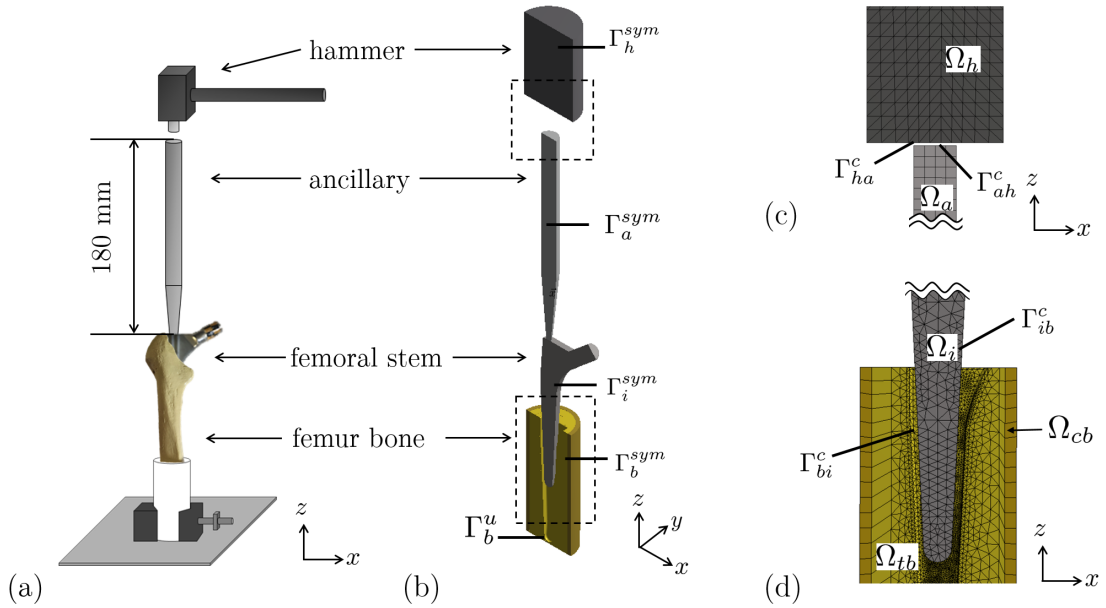

Figure 1: Representation of the experimental setup (a) and the geometry of the different domains for the simulation (b) with zooms on the meshes at the hammer-ancillary contact (c) and at the bone-stem contact (d). The hammer, the ancillary, the FS implant, the trabecular bone and the cortical bone are denoted by Ω_h, Ω_a, Ω_i, Ω_{tb}, Ω_{cb}, respectively.

In this work, all media were modeled as isotropic elastic materials, similarly as what was done in [30, 28, 29]. The material properties associated to each domain are given in Table 1 for the reference case. Each material was assumed to be homogeneous and had the same Poisson's ratio equal to 0.3. The mesh was generated in ANSYS Workbench software (v.20, ANSYS Inc., Canonsburg, PA, USA) and consisted in 89381 tetrahedral elements. The mesh was refined around the bone implant contact. A convergence study on the bone and implant element size h_e and the time increment Δt was conducted for the reference case.

Parameter	Density (g/cm^3)	Young's modulus (GPa)
Hammer	8.3	210
Ancillary	7.85	200
Femoral stem	4.4	113
Cortical bone	1.64	18 [33, 34]
Trabecular bone	0.27	0.2 [28, 35]

Table 1: Material properties of the five subdomains taken from [33, 34, 35, 28]

2.2. FS insertion simulation

All simulations were performed using the ANSYS software (v.20, ANSYS Inc., Canonsburg, PA, USA). To describe the dynamic behavior of the system during the insertion process, large displacement hypothesis was assumed. Therefore, the initial configuration at $t = 0$ described by the point coordinates $\boldsymbol{X}$ was distinguished from a given configuration at a time t described by the point coordinates $\boldsymbol{x} = \boldsymbol{x}(\boldsymbol{X}, t)$.

2.2.1. Boundary, initial and contact conditions

Different boundary conditions were defined for each subdomain, denoted Γ^{sym} for the symmetry condition, Γ^c for the contact condition and Γ^u for the imposed displacement as indicated in Fig. 1. The bone distal surface, Γ^u_b, was fixed to represent the distal bone clamping of the experimental configurations [15, 10]. No external forces were applied to the system. The symmetry condition Γ^{sym} in the (XZ) plane was applied to the whole system, according to the plane of symmetry of the femoral stem. The symmetry boundary conditions read (except for the contact surfaces):

$$\boldsymbol{u} = \boldsymbol{0}, \qquad \text{on } \Gamma_b, \tag{1}$$

$$\boldsymbol{u} \cdot \mathbf{e_y} = 0, \qquad \text{in } \Gamma^{sym}_{\alpha}, \tag{2}$$

where $\boldsymbol{u}(\boldsymbol{X}, t) = \boldsymbol{x} - \boldsymbol{X}$ is the displacement vector and $\Gamma^{sym}_{\alpha} = (\Gamma^{sym}_h \cup \Gamma^{sym}_a \cup \Gamma^{sym}_i \cup \Gamma^{sym}_{tb} \cup \Gamma^{sym}_{cb})$.

Frictional contact model using Coulomb's law [36] was assumed between the hammer and the ancillary noted (Γ^c_{ha},Γ^c_{ah}) (see Fig. 1c) and between the trabecular bone and the FS implant noted (Γ^c_{bi},Γ^c_{ib})(see Fig. 1d), where:

$$f_s = |F_t| - \mu |F_n| \leq 0. \tag{3}$$

$|F_t|$ and $|F_n|$ are the absolute values of tangential and normal components of the interface traction force vector, respectively; μ is the friction coefficient; and f_s is a slip criterion which is negative ($f_s < 0$) when no sliding occurs (sticking) and null ($f_s = 0$) in case of sliding. Using ANSYS

software (v.20, ANSYS Inc., Canonsburg, PA, USA), the Augmented Lagrangian method was employed to solve the problem involving contact with friction. In particular, a friction coefficient of 0.1 was chosen between the hammer and the ancillary, similarly as in [30] and it was chosen equal to 0.3 for the reference case based on previous values used in the literature [37, 30, 28].

To simulate the impact of the hammer Ω_h on the ancillary Ω_i, an initial vertical velocity was imposed to Ω_h at $t = 0$. At $t = 0$, the bone and the implant were supposed to be at rest and already in contact along Γ^c. The initial conditions read:

$$\boldsymbol{u}_{(t=0)} = \mathbf{0}, \qquad \text{in } \Omega_\alpha, \tag{4}$$

$$\dot{\boldsymbol{u}}_{(t=0)} = \mathbf{0}, \qquad \text{in } (\Omega_a \cup \Omega_i \cup \Omega_{tb} \cup \Omega_{cb}), \tag{5}$$

$$\dot{\boldsymbol{u}}_{(t=0)} = (0, 0, -v_0), \qquad \text{in } \Omega_h, \tag{6}$$

where $\dot{\boldsymbol{u}}(\boldsymbol{X}, t)$ is the velocity vector and $\Omega_\alpha = (\Omega_h \cup \Omega_a \cup \Omega_i \cup \Omega_{tb} \cup \Omega_{cb})$.

2.2.2. Impaction procedure and parametric study

Different simulations of the femoral stem insertion by impaction were performed using the numerical model described above. Before starting the impaction procedure, the implant was positioned into the bone cavity to establish the contact between the bone and the implant by applying a quasi-static vertical force of 10N to the upper surface of the ancillary, similarly as what was done in [29]. This stage represents the manual positioning of the implant into the bone performed by the surgeons before the hammer impacts. The insertion procedure by impaction (denoted "implant impaction" in what follows), starts at the end of the implant positioning. It consisted in applying successive impacts of the hammer on the ancillary, with an initial vertical velocity equal to v_0 for each new impact. The number of impacts was set equal to 10 for each simulation (except for $v_0 = 2$ m/s, which will be discussed in Section 4) in order to be able to compare the influence of the configuration on the implant insertion. The time duration between two successive impacts was adapted to each configuration so that the system was at rest at the beginning of each new impact, to ensure consistency of the initial condition across the configurations. Because of the dynamic behavior of the system, this time duration was larger at the beginning of the insertion than at the end.

A parametric study was carried out based on the experimental variations observed in [15, 16, 17] by repeating the protocol described above with different biomechanical configurations. To model

the variability of the patient and of the surgical procedure, different values of trabecular bone Young's modulus E_t, friction coefficient at the bone-implant interface μ, interference fit IF and impact velocity v_0 were considered, leading to a total of 17 simulations. The range of variation of each parameter is indicated in Table 2 and was defined according to both the experimental data taken from the literature and the feedbacks of two experienced orthopedic surgeons. In what follows the reference values of the aforementioned parameters will be denoted by E_t^*, IF^*, μ^* and v_0^*.

Parameter	Symbol	Range	Reference value
Trabecular bone Young's Modulus	E_t	[0.1-0.6] GPa [38, 39, 40]	0.2 GPa [35]
Interference fit	IF	[100-300] µm [41, 21, 42]	200 µm
Friction coefficient	μ	[0.2-0.5] [34, 37, 43]	0.3 [28]
Impact velocity	v_0	[0.5-2] m/s	1 m/s

Table 2: Parameters and range of variation for the parametric study. [38, 39, 40, 35, 41, 21, 42, 34, 37, 43, 28]

2.3. Insertion monitoring and signal processing

To analyze the femoral stem insertion, the positions of the hammer and of the ancillary, the implant vertical displacement U_I, as well as the BIC ratio were evaluated during the impaction procedure. The implant displacement U_I was defined by the variation of the position of the ancillary during each impact $\#i$. The BIC was defined by the ratio of the bone surface in contact with the femoral stem and with the total bone cavity surface. To investigate the impact method sensitivity, the time variation of the impact force F_I applied by the hammer on the upper surface of the ancillary was determined during each impact $\#i$ of the impact procedure. The same signal processing method as the one presented in [15, 16, 17] was employed in order to analyze the impact force signal $s(t)$ measured at the hammer lower surface. An indicator, noted D, was calculated for each impact $\#i$. The indicator D, given in milliseconds, corresponds to the interval between the times t_2 and t_1 of the second and the first local maxima of the signal $s(t)$ respectively (see [15, 17, 16] for more details).

3. Results

3.1. Analysis of the FS insertion: reference case

The variation of the positions of the hammer's impact surface and of the ancillary's upper surface during an impaction procedure composed of ten impacts is shown in Fig. 2 for the reference case ($E_t = E_t^*$, $IF = IF^*$, $\mu = \mu^*$ and $v_0 = v_0^*$. During each impact $\#i$, the hammer bounces

on the ancillary fixed to the femoral stem, which is illustrated by the local minima on the curve representing the hammer position (see Fig. 2). The femoral stem displacement U_I is higher at the beginning of the insertion procedure. The position of the ancillary varies by less than 0.25 mm between each impact after the 6^{th}, which indicates that from a macroscopic perspective, the femoral stem may be considered as almost fully inserted into the host bone.

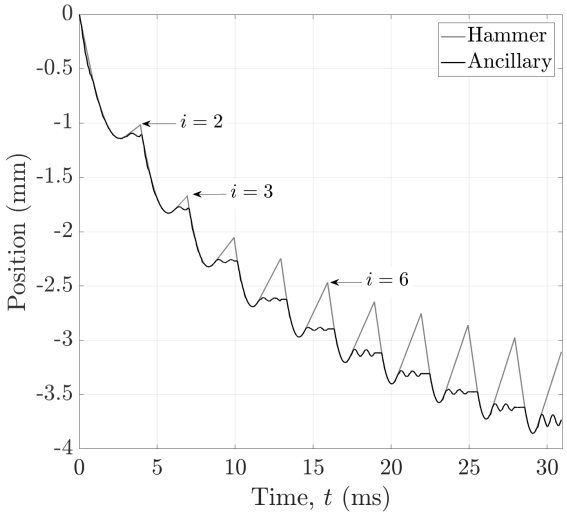

Figure 2: Positions of the hammer impact surface (grey line) and of the ancillary upper surface (black line) along the z-axis obtained during the impaction for the reference case. The origin ($z = 0$) of the ordinate axis corresponds to the position of the upper surface of the ancillary at the end of the contact positioning for the reference case.

Figure 3 shows the spatial variation of the Von Mises stresses in the peri-implant bone tissue after one, three, six and ten impacts realized during the insertion procedure for the reference case. As shown in Fig. 3, the stresses are concentrated around the contact region. First, stresses are localized around the bone-implant interface corresponding to the proximal curvature of the implant (indicated by the circles in Fig. 3 for impact #1) at the beginning of the insertion and then they extend to the distal region after several impacts.

The description of two impacts (#1 and #3) measured during the femoral stem insertion procedure is illustrated in Fig. 4 for the reference case. The variation of the force applied between the hammer and the ancillary as a function of time is shown in Fig. 4a for the impact #1 (respectively in Fig. 4c for the impact #3). The variation of the position of the ancillary and the hammer during the impact #1 (respectively impact #3) is represented in Fig. 4c (respectively 4d). The first peak of the force signals $s(t)$ corresponds to the initial hammer blow on the ancillary. The following peaks represent the rebounds of the ancillary on the hammer. When the curves of the hammer and ancillary positions shown in Figs. 4b and 4d are superposed, $s(t)$ is shown to

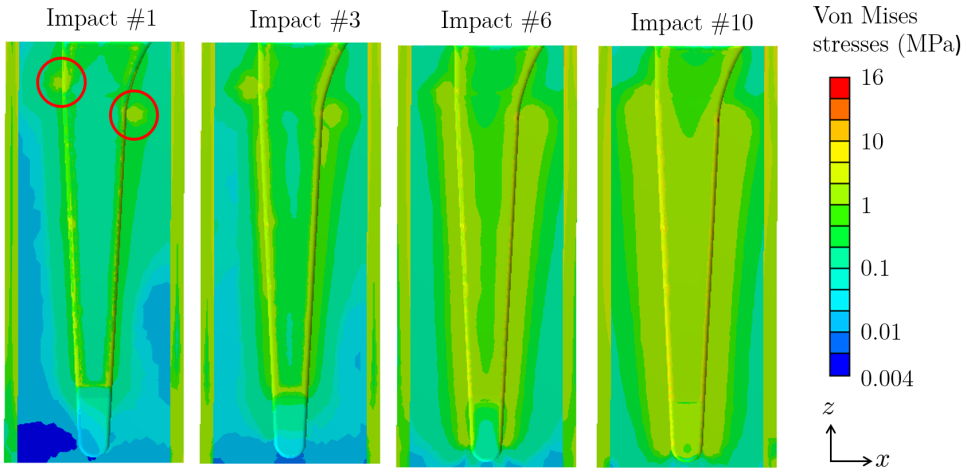

Figure 3: Von Mises stresses in the peri-implant femoral bone after one, three, six and ten impacts for the reference case. The circles indicate the bone area corresponding to the proximal curvature of the implant.

be strictly positive, which corresponds to a rebound of the hammer on the ancillary. The time difference between the initial hammer blow (peak #1) and the first rebound of the ancillary on the hammer (peak #2) varies throughout the impaction procedure. The time of the second peak is around 0.9 ms for the impact #1 (see Fig. 4a) and 0.5 ms for the impact #3 (see Fig. 4c).

Several examples of the signal $s(t)$ corresponding to the variation of the impact force as a function of time measured between the hammer and the ancillary are shown in Fig. 5 for different impacts $\#i$ during the insertion procedure for the reference case. The impact number $\#i$ is indicated above each second peak of the force signal $s(t)$. The value of the time difference described in Fig. 4 and defined as the indicator D [15, 16, 17] decreases during the implant impaction procedure. In particular, the variation of the indicator D as a function of the impact number $\#i$ is shown in Fig. 6 for the reference case, together with femoral stem displacement U_I (Fig. 6a) and the BIC ratio (Fig. 6b). The time difference D first decreases as a function of the impact number $\#i$ and then stays constant and equal to around 0.23 ms after seven impacts. The total implant displacement after 10 impacts is around 4 mm for the reference case (see Fig. 2). Note that the implant displacement is calculated from the beginning of the impaction procedure, once the implant is positioned inside the bone cavity. The implant displacement U_I is higher at the beginning of the impaction procedure than at the end. Even if the displacement still varies after the impact #10, the variation of U_I between the impacts #10 and #9 is about 0.25 mm, which is much smaller than its variation about 0.75 mm between the impacts #1 and #2 (see Fig. 2 and 6). Similarly, 80% of the BIC ratio is reached after the four first impacts. The BIC ratio only

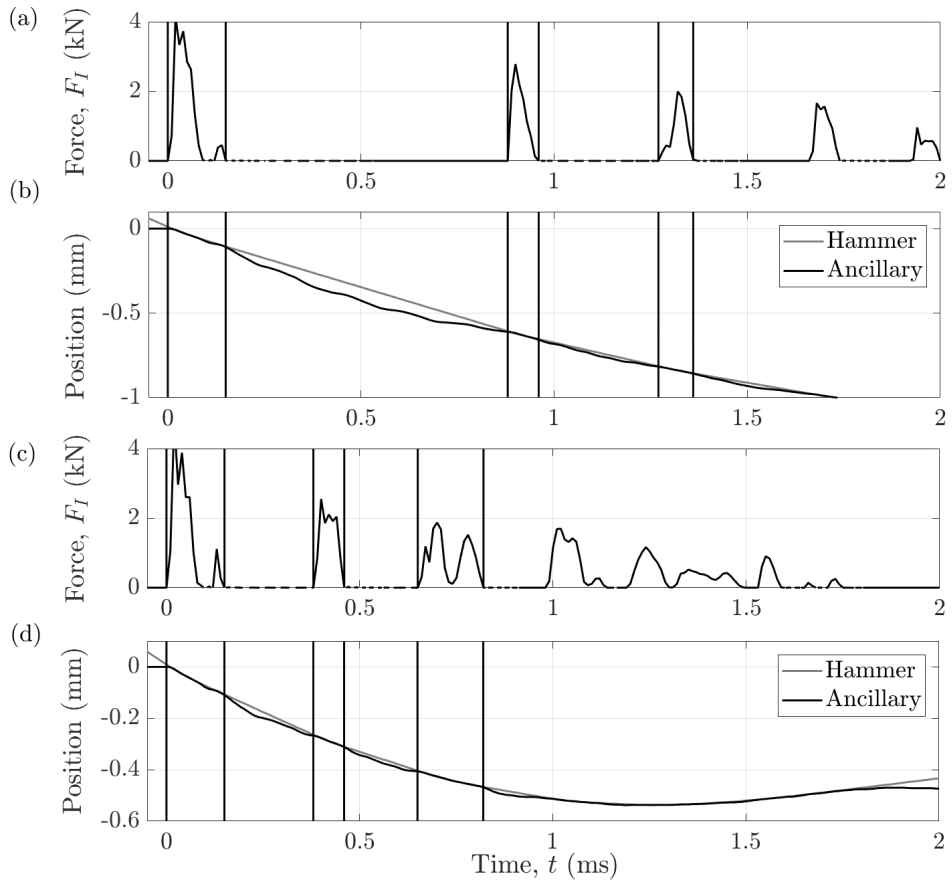

Figure 4: Description of the impact realized during femoral stem insertion for the reference case. a) (respectively c): force measured at the hammer lower surface and b) (respectively d) positions of the hammer and of the ancillary along the z-axis during the impact #1 (respectively impact #3).

224 increases from 10% for the six last impacts.

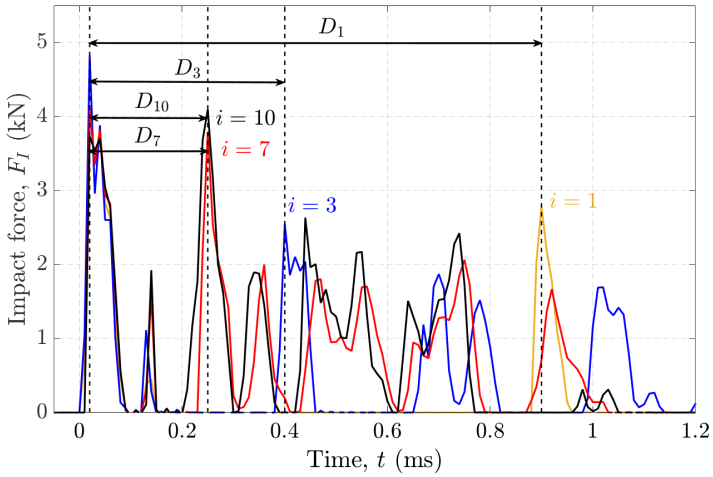

Figure 5: Illustration of signals $s(t)$ corresponding to the variation of the force as a function of time measured during different impacts $\#i$ applied to the ancillary to insert the femoral stem into the bone for the reference case.

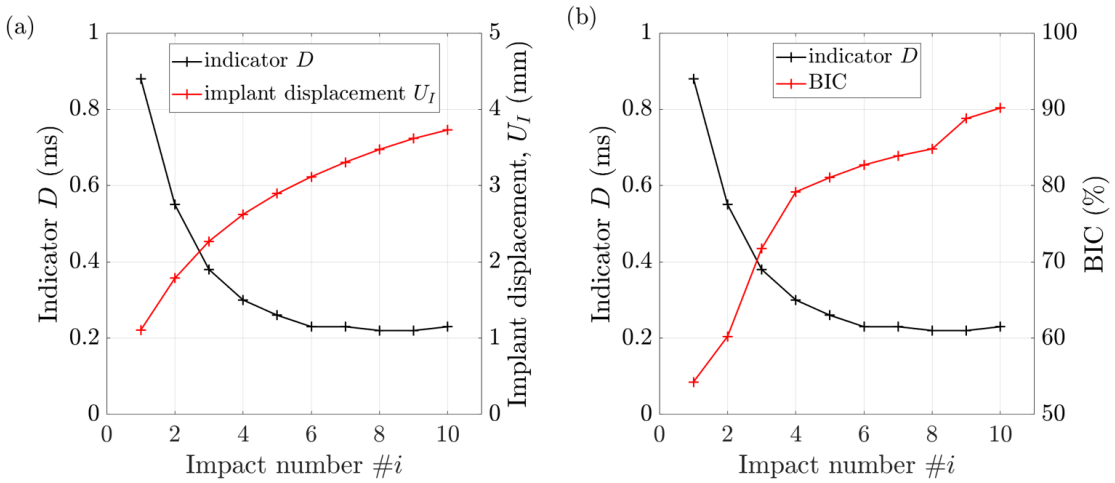

Figure 6: Variation of the indicator D, the implant displacement U_I (a) and the BIC ratio (b) as a function of the impact number $\#i$ during the femoral stem insertion procedure for the reference case.

3.2. Influence of the environment on the FS insertion: a parametric study

Figure 7 shows the influence of the trabecular bone Young's modulus E_t, the friction coefficient μ, the impact velocity v_0 and the interference fit IF on the BIC ratio as a function of the impact number $\#i$. The values of the BIC ratio always increase during the femoral stem insertion procedure for all values of E_t (a), μ (b), v_0 (c) and IF (d). Except for the case $E_t = 600$ MPa (see Fig. 7, which will be discussed in Section 4), the increase of the BIC ratio is higher at the beginning of the impaction procedure and the BIC asymptotically reaches a threshold value during the impaction procedure. The number of impacts necessary to obtain the threshold depends on the configuration and is smaller for the lowest values of E_t, μ and IF and for the highest values of v_0.

Overall, for any impact number $\#i$, the BIC ratio increases when E_t, μ, IF decrease and when the impact velocity v_0 increases (see Fig. 7). The BIC ratio reached at the end of insertion ($i = 10$) varies between 74% and 97% according to the value of E_t, between 81% and 96% according to the value of μ, between 60% and 98% according to the value of v_0 and between 81% and 91% according to the value of the interference fit IF. A difference of BIC ratio of 40% is obtained after the tenth impact for the two extreme values of impact velocities considered herein: $v_0 = 0.5$ m/s and $v_0 = 1$ m/s (Fig. 7c). In particular, the BIC ratio corresponding to $v_0 = 0.5$ m/s does not significantly increase after the 7^{th} impact, which may be explained by insufficient tangential forces at the bone-implant interface produced by an impact with $v_0 = 0.5$ m/s compared to the normal forces. For $v_0 = 0.5$ m/s, it may be hypothesized that continuing the impaction procedure with such velocity would not lead to an increase of the BIC ratio.

Figure 8 shows the variation of the indicator D as a function of the BIC ratio during the femoral

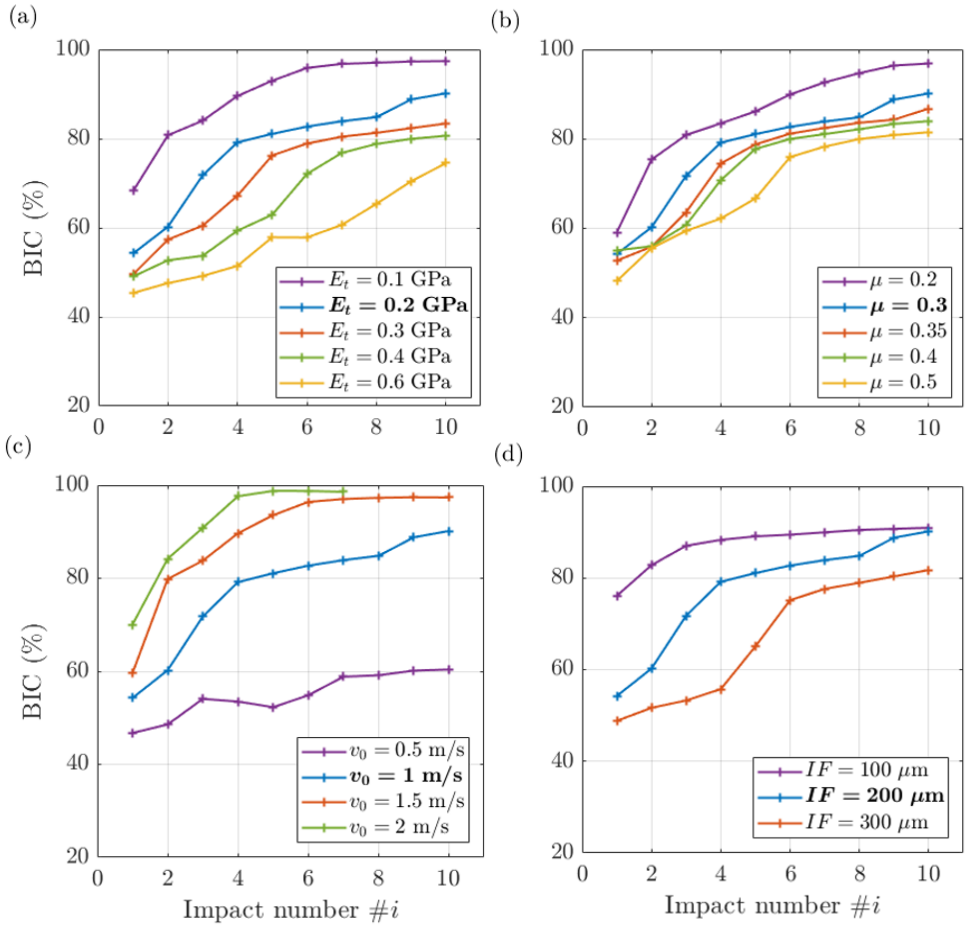

Figure 7: Variation of the BIC ratio as a function of the impact number $\#i$ during the femoral stem insertion procedure into the bone. The results are presented for different values of the trabecular bone Young's modulus (a), friction coefficient μ (b), impact velocity v_0 (c) and interference fit IF (d). When one parameter is investigated, the others are set to their reference values. The reference case is highlighted in bold in the legend.

stem insertion for different values of trabecular bone Young's modulus E_t (a), friction coefficient μ (b), impact velocity v_0 (c) and interference fit IF (d). For any value of E_t, IF, μ, and v_0, the indicator D first decreases as a function of the BIC ratio and then remains constant at a value close to 0.23 ms. The value of the BIC ratio corresponding to the convergence of D varies from 60 % to 95 % according to the configuration. This value is smaller for higher trabecular bone Young's modulus E_t (see Fig. 8a), higher friction coefficient μ (see Fig. 8b) and higher interference IF (see Fig. 8d) and for smaller impact velocity v_0 (see Fig. 8c).

4. Discussion

The aim of the present study is to provide more physical insights on the dynamic phenomena occurring during the femoral stem insertion of the impaction procedure under various biomechanical

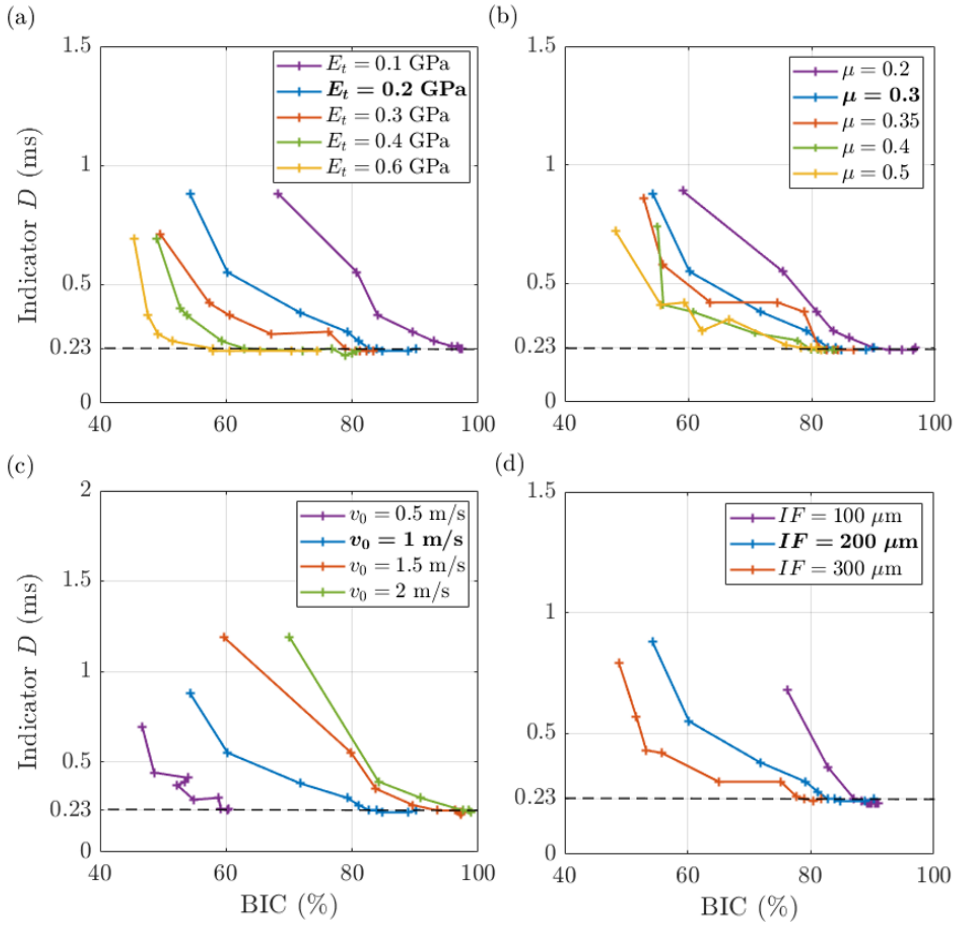

Figure 8: Variation of the indicator D as a function of the BIC ratio during the femoral stem insertion procedure into the bone. The results are presented for different values of the trabecular bone Young's modulus E_t (a), friction coefficient μ (b), impact velocity v_0 (c) and interference fit IF (d). When one parameter is investigated, the others are set to their reference values. The reference case is highlighted in bold in the legend.

configurations. From the best of the author's knowledge, this is the first work that analyzes the impact force during the femoral stem insertion using a 3D finite element model. In particular, the time indicator D [15, 17, 16], derived from the impact force signal is studied during the femoral stem insertion and its sensitivity to the biomechanical configuration is investigated. Moreover, the originality of the work is to analyze the influence of specific parameters on the impaction protocol and on the implant stability, such as the bone Young's Modulus, the interference fit, the friction coefficient and the impact velocity, which had not all been studied so far [32, 31]. The findings of this study and the use of impact analysis to monitor implant insertion are of interest to improve not only the primary stability but also the long-term success of the implant, since it highly depends on the stability achieved during the impaction protocol [44].

4.1. *Influence of the parameters on the implant insertion and stability*

The maximum value of the BIC ratio achieved during femoral stem insertion as well as the number of hammer impacts necessary to reach this value, were shown to strongly depend on the value of E_t, which is related to the patient's bone tissue quality and on IF, μ and v_0, which are related to the surgical configuration (see Fig. 7). This observation confirms the importance to adapt the surgical procedure to maximize the implant stability [5, 31, 28]. The BIC ratio first increases with the impact number and then stays constant. A similar behavior was observed in [29] where the quasi-static insertion force is representative of the cumulative impacts in the study herein. The number of impacts necessary to reach the maximal BIC value is higher when the bone-implant system stiffness is higher, that is for higher values of E_t, μ and IF. Considering a high value of $E_t = 600$ MPa, the BIC ratio still increases after the 10^{th} impact, which indicates that the implant can not be fully inserted and the primary stability could not be optimized. The non-linear evolution of the bone-implant contact ratio during the insertion procedure as well as the influence of the friction coefficient on the BIC ratio are in agreement with the results found in the study of Monea et al. [32]. However, the values of the maximal BIC ratio are higher in the present study than in [32], which may be due to differences of implant geometries or of interference fit values and which does not allow a quantitative comparison of the results.

The present parametric study reveals that for low initial velocity of the hammer ($v_0 = 0.5$ m/s), applying additional impacts with the same intensity does not lead to an increase of the BIC ratio, even for relatively low BIC ratio values (around 60%). This result confirms the importance of considering the impact force, which is related to the initial velocity of the hammer v_0, to maximize implant stability [45, 31, 46].

Contrarily to the case of the ACI where the stress field was concentrated around the equatorial rim [27, 28, 30], more regular distributions of the stress field at the peri-implant bone zone were obtained (see Fig. 3), which may be explained by the large contact surfaces between the femoral stem and the bone. Note that the level of Von Mises stresses computed by the present model is consistent with the results obtained by Monea et al. [32], comprised between [1-20] MPa.

These results on the influence of the various parameters on the bone-implant contact are difficult to validate experimentally, because i) it is not possible to measure the bone-implant contact ratio during the implant insertion and ii) it is difficult to vary each parameter independently. Although imaging techniques could be used, the presence of artefacts around the implant would prevent from a quantitative measurement at the bone-implant interface. Moreover, it is difficult to control the

geometry and the size of the bone cavity as precisely as in a numerical model.

Overall, some recommendations may be provided to the surgeons to improve bone-implant contact, based on the influence of the trabecular bone Young's modulus, the friction coefficient, the interference and the impact velocity on the implant insertion (see Fig. 7). First, the surgeon should adapt the number of impacts depending on the bone quality: the lower is the bone Young's modulus, the lower is the number of impacts required to reach a given bone-implant contact. Second, the choice of a lower press-fit conditions (*i.e.* IF values) and a lower friction coefficient (*i.e* μ values) allows to reach higher bone-implant contact for a given number of impact. Third, the impact velocity should be high enough to reach a sufficient bone-implant contact. Based on the findings for the reference case (see Fig. 7c) the impact velocity should be higher than 0.5 m/s. In addition, the higher is the velocity, the lower is the number of impacts necessary to reach a given bone-implant contact value.

4.2. Impact force analysis

The time signal of the impact force measured between the hammer and the ancillary, which is illustrated in Fig. 4 for different impacts in the reference case, is qualitatively similar to the experimental signals obtained in previous *in vitro* [15, 10] and *ex vivo* studies [17, 16]. In these experimental studies, the signal was measured by a piezoelectric force sensor fixed on the hammer's impact surface. The numerical model allows to precisely compare the impact force signal and in particular, the time and duration of the peaks with the positions of the ancillary and the hammer, which is more difficult experimentally. The analysis of the impact confirms that the peaks following the initial hammer impact correspond to the successive rebounds of the ancillary on the hammer (see Fig. 4). For any value of trabecular bone Young's modulus E_t, friction coefficient μ, interference fit IF and impact velocity v_0 in the ranges considered herein, it was verified that the impact force signal was always made up of several successive peaks (data not shown). In the literature, other numerical and experimental studies, mostly focused on the acetabular cup implant [47, 30] found that the ancillary, which is fixed to the uncemented implants, "rebounds" on the hammer during the insertion procedure, which is coherent with the temporal variation of the force signal observed with the present numerical model (see Fig. 2). Michel et al. [30] studied the AC implant insertion by means of a 2D axi-symmetric model. While a similar behavior of the impact force signal was obtained in the present study, the bone-implant contact evolution could not be compared because of the difference of geometry.

The time duration between the impact and the first rebound, named indicator D, first, decreases as a function of the impact number and then, reaches a threshold and stays constant (see Fig. 6). This behavior was also observed experimentally in previous studies with bone mimicking samples [15, 10] bovine bone sample [16] and anatomical subjects [17], a situation closed to the operating room, allowing for the definition of an insertion end-point criterion based on the convergence of the indicator. However, these studies did not investigate the variation of the indicator as a function of the bone-implant contact, as it is not possible to measure such quantity during the insertion. In previous numerical works on press-fitted implants, Michel et al. [30] and Bishop et al. [48, 31] also showed that the time variation of the impact force signal provides information on the implant stability for the acetabular cup implant and the femoral stem, respectively. However, the difference of the configuration (implant geometry, bone anatomy) with Michel et al. [30] and Bishop et al. [48, 31] does not allow to compare the different studies quantitatively. In the present study, the insertion end-point criterion based on the convergence of the indicator D was shown to be in good agreement with the surgeon proprioception and the implant insertion depth. The present parametric study proves that the indicator D converges to 0.23 ms for any value of E_t, μ, IF and v_0 (see Figure 8). However, for several configurations, the BIC ratio continues to increase after D reaches this threshold of 0.23 ms. The number of impacts needed for D to converge towards its threshold (0.23 ms) is lower when the bone-implant system rigidity is higher (*i.e* higher trabecular bone Young's modulus E_t, friction coefficient μ and interference fit IF). In addition, the BIC ratio corresponding to the convergence of D is lower when considering a higher bone-implant system rigidity. This result reveals that the indicator D is not directly correlated to the BIC ratio but rather to the global stiffness of the bone-implant system. Therefore, the pull-out force, which was shown to increase as a function of the bone-implant rigidity [29], could also be used (in addition to the BIC ratio) to evaluate the sensitivity of the indicator D to the femoral stem stability. It is worth noting that the implant displacement produced from the last impacts of the impaction procedure, for which the indicator D stays constant, is smaller than 0.25 mm (see Fig. 6 for the reference case), which is too low to be measurable in the clinic and may be neglected.

Although the variation of the indicator D as a function of the impact number is in good qualitative agreement with previous experimental studies, the value of the convergence threshold slightly differs. It was shown herein that the indicator D converges to 0.23 ms for any value of E_t, μ, IF and v_0. However, experimental results showed that the indicator D reached a threshold comprised between 0.4 and 0.6 ms according to the type of the bone (femur mimicking phantoms

[15], bovine femur bone [16] or human bone [17]). Multiple factors can explain this difference. First, the material properties considered in the model are not fully representative to the real materials. In particular, while bone tissue behaves as a viscoelastic material [49, 50], only elastic materials are considered in the present model, which does not account for dissipation mechanisms. Note that this assumption has already been made in previous similar modeling approaches [30, 28]. Second, the boundary conditions at the distal femur do not exactly reproduce the clamping nor the anatomical conditions considered in the experimental configurations, which is likely to modify the resonance of the bone-implant system and therefore the time duration between the rebound of the ancillary on the hammer. Eventually, a cylinder represents the femoral bone, which differs from a real femur anatomy especially in the proximal part and may also influence the stiffness of the bone-implant system, and thus, the number of impacts necessary to insert the implant and the corresponding value of the time indicator.

Overall, this study confirms that impact analysis is a promising non-invasive method to monitor implant insertion (see Fig. 6 and 8), which supports the previous experimental findings [15, 17, 16] and open the path towards a clinical study. However, this numerical study rises a limitation concerning the sensitivity of the indicator D derived from the impact force signal, which no longer varies for small changes of BIC ratio at the end of insertion. Therefore, the method could be coupled with other monitoring methods studied in the literature such as vibration analysis [29, 10, 51] or acoustic methods [8].

4.3. Limitations and perspectives

The finite element model developed in this study presents several limitations in addition to the ones mentioned above. First, the geometrical configuration differs between the experimental and numerical approaches. The thickness of the cortical bone was modeled as a uniform layer of 3.5 mm whereas it is actually non-uniform. Nonetheless, since the femoral stem is only in contact with trabecular bone in the model herein, the uniform cortical bone thickness is not expected to significantly influence the results. Moreover, an "ideal" bone cavity is modeled, whereas it was shown that the cavity reaming may vary between surgeons [52]. The cavity reaming as well as the impact direction may influence the femoral stem insertion into the bone [53]. In particular, the femoral stem implant is perfectly aligned to the bone cavity at the beginning of insertion and the impact force is purely vertical. However, the horizontal displacements along the x-direction are allowed in our model. Eventually, it would also be relevant to consider other implant geometries,

since it is expected to influence the evolution of the bone-implant contact ratio as a function of the impact number. Nonetheless, the stem type used in this study is largely employed for uncemented surgeries, due to the cervico diaphyseal angle of 132° and the medial curvature adapted to different morphologies [54], which confirms the relevance of the results obtained herein for most uncemented procedures.

Second, bone tissue is known to exhibit viscoelastic, anisotropic [55] and heterogeneous [33] properties. However, homogeneous, isotropic and elastic materials were assumed for all configurations considered throughout this study because it allows to change only one parameter (Bone Young's Modulus) rather than an important number if a more realistic assumption was made. Heterogeneous and patient specific bone properties could be taken into account using CT scans to recover the bone anatomy along with the spatial distribution of the bone density [56, 57, 58, 59]. The anisotropy [60, 55] of the trabecular bone could also be investigated, together with its viscoelastic behavior, which is out of the scope of the present work. The aim of the present study was to investigate the influence of several parameters which are difficult to determine and control experimentally on the phenomena occurring during femoral stem insertion. For that purpose, we assumed a simplified material model for the parametric study, where only the global stiffness of the bone was considered via the Young's modulus and neglecting the anisotropic bone properties [60], to simplify the comparison between the different configurations. Overall, the comparison between the different configurations should not be affected by this assumption, which was made consistently for all of them.

Third, plastic deformations [61], as well as bone damage [48, 62] and bone compaction [53, 63] are likely to occur in the peri-implant bone tissue during its insertion, which may affect the bone cavity geometry and the bone stiffness. Because of the important stress field generated when inserting the implant, significant fluid circulation in the bone porosities may occur [64], which could also affect the acoustical response of the bone-implant system. These phenomena, which could be modeled through bone damage modeling or coupling with computational fluid dynamics, were not taken into account in the present work as it was assumed that they affect less the impact force signal than the range of parameters chosen in the parametric study. Moreover, the value of the Von Mises stresses in the peri-implant bone (see Fig. 3) at the end of insertion remains inferior to the tensile and compression yield stresses of the bone reported in the literature [65, 39, 66].

In future works, it will be relevant to go deeper into the development of patient specific models. Towards this goal, neural networks (*e.g.* siamese networks) could help taking into account even

more parameters related to both the patient and the surgical procedures than the ones studied in the present work. Such analysis could provide more insights on their influence on the implant insertion and stability. In addition, data fusion techniques could allow combining information from various available sources including for instance: the force sensor, medical imaging and the surgeon proprioception. This last point could provide a more comprehensive understanding of the influence of the biomechanical environment on the implant stability and the impact analysis. Thereby, artificial intelligence could help not only, to predict primary stability but also secondary stability. Because of the wide variations observed in the clinic among patients and surgical protocols, these techniques are of great interest to improve patient outcomes and to progress towards the use of per-operative impact-based methods to optimize the implant insertion procedure.

5. Conclusion

In the present study, a 3-D finite element model of the femoral stem impaction into the bone is proposed to provide more physical insights on the dynamic phenomena occurring during uncemented implant insertion. The femoral stem insertion is studied in terms of implant displacement, bone-implant contact ratio and impact force for various values of bone properties, interference fit, bone-implant-contact friction coefficient and impact velocity. The results emphasize the necessity to adapt the number and velocity of the impacts depending on the biomechanical configuration to reach a satisfying BIC ratio. The impact force is shown to vary during the impaction procedure. A time indicator D is derived from the impact force signal based on previous experimental studies. This indicator corresponds to the time difference between the initial hammer impact and the rebound of the ancillary on the hammer. The indicator D decreases with the impact number and converges to a threshold value of 0.23 ms, independently of the biomechanical configuration. Based on the results of this study, this indicator could be used experimentally to retrieve a macroscopic bone-implant stiffness. Since this indicator allows real-time monitoring based on the temporal variation of the impact force only, this approach could be employed during the impaction procedure to guide the surgeon to optimize implant insertion.

6. Acknowledgments

This project has received funding from the European Research Council (ERC) under the European Union's Horizon 2020 research and innovation program (grant agreement No 682001, project ERC Consolidator Grant 2015 BoneImplant and grant agreement No 101062467, project ERC

Proof of Concept 2021 Impactor), from the project OrthAncil (ANR-21-CE19-0035-03) and from the project OrthoMat (ANR-21-CE17-0004).

7. Declaration of Conflicting Interests

The authors declare that they have no financial or non-financial interests that are directly or indirectly related to the work submitted for publication.

8. Data availability

The data may be available upon reasonable request.

References

[1] Putman S, Girier N, Girard J, Pasquier G, Migaud H, Chazard E. Épidémiologie des prothèses de hanche en France : analyse de la base nationale du PMSI de 2008 à 2014. Revue de Chirurgie Orthopédique et Traumatologique. 2017 Nov;103.

[2] Zarychta P. A new approach to knee joint arthroplasty. Computerized Medical Imaging and Graphics. 2018 Apr;65:32-45.

[3] Kelmer G, Stone AH, Turcotte J, King PJ. Reasons for Revision: Primary Total Hip Arthroplasty Mechanisms of Failure. JAAOS - Journal of the American Academy of Orthopaedic Surgeons. 2021 Jan;29(2):78.

[4] Apostu D, Lucaciu O, Berce C, Lucaciu D, Cosma D. Current methods of preventing aseptic loosening and improving osseointegration of titanium implants in cementless total hip arthroplasty: a review. Journal of International Medical Research. 2018 Jun;46(6):2104-19.

[5] Doyle R, van Arkel RJ, Muirhead-Allwood S, Jeffers JRT. Impaction technique influences implant stability in low-density bone model. Bone & Joint Research. 2020 Jul;9(7):386-93.

[6] Ulrich SD, Seyler TM, Bennett D, Delanois RE, Saleh KJ, Thongtrangan I, et al. Total hip arthroplasties: What are the reasons for revision? International Orthopaedics. 2008 Oct;32(5):597-604.

[7] Bissias C, Kaspiris A, Kalogeropoulos A, Papoutsis K, Natsioulas N, Barbagiannis K, et al. Factors affecting the incidence of postoperative periprosthetic fractures following primary and revision hip arthroplasty: a systematic review and meta-analysis. Journal of Orthopaedic Surgery and Research. 2021 Jan;16(1):15.

[8] Goossens Q, Pastrav L, Roosen J, Mulier M, Desmet W, Vander Sloten J, et al. Acoustic Analysis to Monitor Implant Seating and Early Detect Fractures in Cementless Tha: An in Vivo Study. Journal of Orthopaedic Research: Official Publication of the Orthopaedic Research Society. 2020 Aug.

[9] Pastrav LC, Jaecques SV, Jonkers I, Perre GVd, Mulier M. In vivo evaluation of a vibration analysis technique for the per-operative monitoring of the fixation of hip prostheses. Journal of Orthopaedic Surgery and Research. 2009 Apr;4:10.

[10] Poudrel AS, Rosi G, Nguyen VH, Haiat G. Modal Analysis of the Ancillary During Femoral Stem Insertion: A Study on Bone Mimicking Phantoms. Annals of Biomedical Engineering. 2022 Jan;50(1):16-28.

[11] Michel A, Bosc R, Mathieu V, Hernigou P, Haiat G. Monitoring the press-fit insertion of an acetabular cup by impact measurements: Influence of bone abrasion. Proceedings of the Institution of Mechanical Engineers, Part H: Journal of Engineering in Medicine. 2014 Oct;228(10):1027-34.

[12] Michel A, Bosc R, Vayron R, Haiat G. In Vitro Evaluation of the Acetabular Cup Primary Stability by Impact Analysis. Journal of Biomechanical Engineering. 2015 Mar;137(3):031011.

[13] Michel A, Bosc R, Sailhan F, Vayron R, Haiat G. Ex vivo estimation of cementless acetabular cup stability using an impact hammer. Medical Engineering & Physics. 2016 Feb;38(2):80-6.

[14] Michel A, Bosc R, Meningaud JP, Hernigou P, Haiat G. Assessing the Acetabular Cup Implant Primary Stability by Impact Analyses: A Cadaveric Study. PLOS ONE. 2016 Nov;11(11):e0166778.

[15] Tijou A, Rosi G, Vayron R, Lomami HA, Hernigou P, Flouzat-Lachaniette CH, et al. Monitoring cementless femoral stem insertion by impact analyses: An in vitro study. Journal of the Mechanical Behavior of Biomedical Materials. 2018 Dec;88:102-8.

[16] Albini Lomami H, Damour C, Rosi G, Poudrel AS, Dubory A, Flouzat-Lachaniette CH, et al. Ex vivo estimation of cementless femoral stem stability using an instrumented hammer. Clinical Biomechanics. 2020 Jun;76:105006.

[17] Dubory A, Rosi G, Tijou A, Lomami HA, Flouzat-Lachaniette CH, Haïat G. A cadaveric validation of a method based on impact analysis to monitor the femoral stem insertion. Journal of the Mechanical Behavior of Biomedical Materials. 2019 Nov;103:103535.

[18] Reimeringer M, Nuño N. The influence of contact ratio and its location on the primary stability of cementless total hip arthroplasty: A finite element analysis. Journal of Biomechanics. 2016 May;49(7):1064-70.

[19] Russell RD, Huo MH, Rodrigues DC, Kosmopoulos V. Stem geometry changes initial femoral fixation stability of a revised press-fit hip prosthesis: A finite element study. Technology and Health Care: Official Journal of the European Society for Engineering and Medicine. 2016 Nov;24(6):865-72.

[20] Pettersen SH, Wik TS, Skallerud B. Subject specific finite element analysis of implant stability for a cementless femoral stem. Clinical Biomechanics. 2009 Jul;24(6):480-7.

[21] Rothstock S, Uhlenbrock A, Bishop N, Morlock M. Primary stability of uncemented femoral resurfacing implants for varying interface parameters and material formulations during walking and stair climbing. Journal of Biomechanics. 2010 Feb;43(3):521-6.

[22] Reimeringer M, Nuño N, Desmarais-Trépanier C, Lavigne M, Vendittoli PA. The influence of uncemented femoral stem length and design on its primary stability: a finite element analysis. Computer Methods in Biomechanics and Biomedical Engineering. 2013;16(11):1221-31.

[23] Dopico-González C, New AM, Browne M. Probabilistic finite element analysis of the uncemented hip replacement–effect of femur characteristics and implant design geometry. Journal of Biomechanics. 2010 Feb;43(3):512-20.

[24] Hennicke NS, Kluess D, Sander M. Influence of stem design parameters on periprosthetic femoral fractures examined by subject specific finite element analyses. Medical Engineering & Physics. 2023 Sep;119:104032.

[25] Gebert A, Peters J, Bishop NE, Westphal F, Morlock MM. Influence of press-fit parameters on the primary stability of uncemented femoral resurfacing implants. Medical Engineering & Physics. 2009 Jan;31(1):160-4.

[26] Folgado J, Fernandes PR, Jacobs CR, Pellegrini VD. Influence of femoral stem geometry, material and extent of porous coating on bone ingrowth and atrophy in cementless total hip arthroplasty: an iterative finite element model. Computer Methods in Biomechanics and Biomedical Engineering. 2009 Apr;12(2):135-45.

[27] Raffa ML, Nguyen VH, Tabor E, Immel K, Housset V, Flouzat-Lachaniette CH, et al. Dependence of the primary stability of cementless acetabular cup implants on the biomechanical environment. Proceedings of the Institution of Mechanical Engineers Part H, Journal of Engineering in Medicine. 2019 Dec;233(12):1237-49.

[28] Immel K, Nguyen VH, Dubory A, Flouzat–Lachaniette CH, Sauer RA, Haïat G. Determinants of the primary stability of cementless acetabular cup implants: A 3D finite element study. Computers in Biology and Medicine. 2021 Aug;135:104607.

[29] Poudrel AS, Nguyen VH, Rosi G, Haiat G. Influence of the biomechanical environment on the femoral stem insertion and vibrational behavior: a 3-D finite element study. Biomechanics and Modeling in Mechanobiology. 2022 Dec.

[30] Michel A, Nguyen VH, Bosc R, Vayron R, Hernigou P, Naili S, et al. Finite element model of the impaction of a press-fitted acetabular cup. Medical & Biological Engineering & Computing. 2017 May;55(5):781-91.

[31] Bishop NE, Wright P, Preutenborbeck M. A parametric numerical analysis of femoral stem impaction. Plos One. 2022 May;17(5).

[32] Monea AG, Pastrav LC, Mulier M, Van der Perre G, Jaecques SV. Numerical simulation of the insertion process of an uncemented hip prosthesis in order to evaluate the influence of residual stress and contact distribution on the stem initial stability. Computer Methods in Biomechanics and Biomedical Engineering. 2014;17(3):263-76.

[33] Goldstein SA. The mechanical properties of trabecular bone: dependence on anatomic location and function. Journal of Biomechanics. 1987;20(11-12):1055-61.

[34] Shirazi-Adl A, Dammak M, Paiement G. Experimental determination of friction characteristics at the trabecular bone/porous-coated metal interface in cementless implants. Journal of Biomedical Materials Research. 1993 Feb;27(2):167-75.

[35] Leuridan S, Goossens Q, Pastrav L, Roosen J, Mulier M, Denis K, et al. Determination of replicate composite bone material properties using modal analysis. Journal of the Mechanical Behavior of Biomedical Materials. 2017;66:12-8.

[36] Wriggers P. Computational contact mechanics. 2nd ed. Berlin ; New York: Springer; 2006.

[37] Damm NB, Morlock MM, Bishop NE. Friction coefficient and effective interference at the implant-bone interface. Journal of Biomechanics. 2015 Sep;48(12):3517-21.

[38] Brown TD, Ferguson AB. Mechanical Property Distributions in the Cancellous Bone of the Human Proximal Femur. Acta Orthopaedica Scandinavica. 1980 Jan;51(1-6):429-37.

[39] Bayraktar HH, Morgan EF, Niebur GL, Morris GE, Wong EK, Keaveny TM. Comparison of the elastic and yield properties of human femoral trabecular and cortical bone tissue. Journal of Biomechanics. 2004 Jan;37(1):27-35.

[40] Metzner F, Neupetsch C, Fischer JP, Drossel WG, Heyde CE, Schleifenbaum S. Influence of osteoporosis on the compressive properties of femoral cancellous bone and its dependence on various density parameters. Scientific Reports. 2021 Jun;11(1):13284.

[41] Abdul-Kadir MR, Hansen U, Klabunde R, Lucas D, Amis A. Finite element modelling of primary hip stem stability: The effect of interference fit. Journal of Biomechanics. 2008 Jan;41(3):587-94.

[42] Sánchez E, de Vries E, Matthews D, van der Heide E, Janssen D. The effect of coating characteristics on implant-bone interface mechanics. Journal of Biomechanics. 2024 Jan;163:111949.

[43] Dammak M, Shirazi-Adl A, Schwartz Jr M, Gustavson L. Friction properties at the bone-metal interface: Comparison of four different porous metal surfaces. Journal of Biomedical Materials Research. 1997;35(3):329-36.

[44] Mathai B, Gupta S. Bone Ingrowth Around an Uncemented Femoral Implant Using Mechanoregulatory Algorithm: A Multiscale Finite Element Analysis. Journal of Biomechanical Engineering. 2021 Sep;144(021004).

[45] Henyš P, Čapek L. Impact Force, Polar Gap and Modal Parameters Predict Acetabular Cup Fixation: A Study on a Composite Bone. Annals of Biomedical Engineering. 2018 Apr;46(4):590-604.

[46] Doyle R, van Arkel RJ, Jeffers JRT. Effect of impaction energy on dynamic bone strains, fixation strength, and seating of cementless acetabular cups. Journal of Orthopaedic Research. 2019 Nov;37(11):2367-75.

[47] Hothi HS, Busfield JJC, Shelton JC. Explicit finite element modelling of the impaction of metal press-fit acetabular components. Proceedings of the Institution of Mechanical Engineers Part H, Journal of Engineering in Medicine. 2011 Mar;225(3):303-14.

[48] Bishop NE, Höhn JC, Rothstock S, Damm NB, Morlock MM. The influence of bone damage on press-fit mechanics. Journal of Biomechanics. 2014 Apr;47(6):1472-8.

[49] Shultz TR, Blaha JD, Gruen TA, Norman TL. Cortical bone viscoelasticity and fixation strength of press-fit femoral stems: finite element model. Journal of Biomechanical Engineering. 2006 Feb;128(1):7-12.

[50] Messer-Hannemann P, Weyer H, Campbell GM, Morlock MM. Time-dependent Viscoelastic Response of Acetabular Bone and Implant Seating during Dynamic Implantation of Press-fit Cups. Medical Engineering & Physics. 2020 Jul;81:68-76.

[51] Pastrav LC, Devos J, Van der Perre G, Jaecques SVN. A finite element analysis of the vibrational behaviour of the intra-operatively manufactured prosthesis-femur system. Medical Engineering & Physics. 2009 May;31(4):489-94.

[52] Konow T, Bätz J, Beverland D, Board T, Lampe F, Püschel K, et al. Variability in Femoral Preparation and Implantation Between Surgeons Using Manual and Powered Impaction in Total Hip Arthroplasty. Arthroplasty Today. 2022 Apr;14:14-21.

[53] Bätz J, Messer-Hannemann P, Lampe F, Klein A, Püschel K, Morlock MM, et al. Effect of cavity preparation and bone mineral density on bone-interface densification and bone-implant contact during press-fit implantation of hip stems. Journal of Orthopaedic Research: Official Publication of the Orthopaedic Research Society. 2019 Jul;37(7):1580-9.

[54] ceraverCerafitRMIS. ceraver Cerafit RMIS HAC; 2020. Available from: https://www.ceraver.com/cerafit-rmis-hac/.

[55] Wirtz DC, Schiffers N, Pandorf T, Radermacher K, Weichert D, Forst R. Critical evaluation of known bone material properties to realize anisotropic FE-simulation of the proximal femur. Journal of Biomechanics. 2000 Oct;33(10):1325-30.

[56] Keller TS. Predicting the compressive mechanical behavior of bone. Journal of Biomechanics. 1994 Sep;27(9):1159-68.

[57] Sansalone V, Naili S, Bousson V, Bergot C, Peyrin F, Zarka J, et al. Determination of the heterogeneous anisotropic elastic properties of human femoral bone: From nanoscopic to organ scale. Journal of Biomechanics. 2010 Jul;43(10):1857-63.

[58] Sansalone V, Bousson V, Naili S, Bergot C, Peyrin F, Laredo JD, et al. Anatomical distribution of the degree of mineralization of bone tissue in human femoral neck: Impact on biomechanical properties. Bone. 2012 Apr;50(4):876-84.

[59] Ovesy M, Voumard B, Zysset P. A nonlinear homogenized finite element analysis of the primary stability of the bone-implant interface. Biomechanics and Modeling in Mechanobiology. 2018 Oct;17(5):1471-80.

[60] Nguyen VH, Rosi G, Naili S, Michel A, Raffa ML, Bosc R, et al. Influence of anisotropic bone properties on the biomechanical behavior of the acetabular cup implant: a multiscale finite element study. Computer Methods in Biomechanics and Biomedical Engineering. 2017 Sep;20(12):1312-25.

[61] Taylor M, Tanner KE, Freeman MA, Yettram AL. Cancellous bone stresses surrounding the femoral component of a hip prosthesis: an elastic-plastic finite element analysis. Medical Engineering & Physics. 1995 Oct;17(7):544-50.

[62] Ovesy M, Aeschlimann M, Zysset PK. Explicit finite element analysis can predict the mechanical response of conical implant press-fit in homogenized trabecular bone. Journal of Biomechanics. 2020 Jun;107:109844.

[63] Zobel SM, Ruhr M, Neumann F, Huber G, Morlock MM. Densification of cancellous bone with autologous particles can enhance the primary stability of uncemented implants by increasing the interface friction coefficient. Journal of Biomechanics. 2022 Jun;139:111149.

[64] Rohan E, Naili S, Cimrman R, Lemaire T. Multiscale modeling of a fluid saturated medium with double porosity: Relevance to the compact bone. Journal of the Mechanics and Physics of Solids. 2012 May;60(5):857-81.

[65] Morgan EF, Keaveny TM. Dependence of yield strain of human trabecular bone on anatomic site. Journal of Biomechanics. 2001 May;34(5):569-77.

[66] Mirzaali MJ, Schwiedrzik JJ, Thaiwichai S, Best JP, Michler J, Zysset PK, et al. Mechanical properties of cortical bone and their relationships with age, gender, composition and microindentation properties in the elderly. Bone. 2016 Dec;93:196-211.